J. Basic. Appl. Sci. Res., 3(10)402-415, 2013

ISSN 2090-4304
Journal of Basic and Applied Scientific Research
www.textroad.com

Effects of a Longitudinal Magnetic Field and Discrete Isoflux Heat Source Size on Natural Convection inside a Tilted Sinusoidal Corrugated Enclosure

Ahmed Kadhim Hussein[1,*], Salam Hadi Hussein[1], Sumon Saha[2], Goutam Saha[3] and M. Hasanuzzaman[4]

[1]Department of Mechanical Engineering, College of Engineering, University of Babylon, Babylon Province, Iraq
[2]Department of Mechanical Engineering, University of Melbourne, VIC 3010, Australia
[3]Department of Mathematics, University of Dhaka, Dhaka-1000, Bangladesh
[4] UM Power Energy Dedicated Advanced Centre (UMPEDAC), Level 4, Wisma R&D, University of Malaya, 59990 Kuala Lumpur, Malaysia

Received: August 3 2013
Accepted: September 1 2013

ABSTRACT

The main objective of this paper is to study numerically a two-dimensional, steady and laminar viscous incompressible magneto-hydrodynamic (MHD) natural convection flow in a sinusoidal corrugated inclined enclosure. In this analysis, two sinusoidal corrugated side walls are maintained at a constant low temperature whereas a constant heat flux source whose length is varied from 20% to 80% of the total length of the enclosure is discretely embedded at the bottom wall. The finite volume method has been used to solve the governing Navier-Stokes and energy conservation equations of the fluid medium in the enclosure in order to investigate the effects of the variation of inclination angles, the presence of a longitudinal magnetic field and different discrete heat source size ratios on heat transfer process for different values of Rayleigh and Hartmann numbers. Results are presented in the form of streamline and isotherm plots. It is concluded that the average Nusselt number increases as the heat surface length decreases and vice versa, while the enclosure inclination angle has a clear effect on the heat transfer process for low heat source lengths in case of low buoyancy and magnetic effects. The dominance of Hartmann number is found to be significant with the purpose of reducing heat transfer process as well as minimizing the influence of inclination angles at low Rayleigh number.

KEYWORDS: Magnetohydrodynamic natural convection, longitudinal magnetic field, tilted corrugated enclosure, isoflux heat source, Hartmann number.

Nomenclature

B_o	magnitude of the magnetic field [T]
g	gravitational acceleration [ms^{-2}]
Ha	Hartmann number
k	thermal conductivity of fluid [$Wm^{-1}K^{-1}$]
L	length of the heat source [m]
Nu	average Nusselt number
p	pressure [Nm^{-2}]
P	dimensionless pressure
Pr	Prandtl number
q	heat flux [Wm^{-2}]
Ra	Rayleigh Number
T	temperature [K]
T_c	temperature of the cold surface (K)
u, v	velocity components in x and y-direction [ms^{-1}]
U, V	dimensionless velocity components in X, Y-direction
W	length of the enclosure [m]
X, y	Cartesian co-ordinates [m]
X, Y	dimensionless Cartesian co-ordinates
Greek symbols	
α	thermal diffusivity [m^2s^{-1}]
β	coefficient of volumetric thermal expansion [K^{-1}]
ε	discrete heat source size ratio
θ	dimensionless temperature
μ	dynamic viscosity of fluid [$kgm^{-1}s^{-1}$]
ρ	density of fluid [kgm^{-3}]
σ_e	electric conductivity [Sm^{-1}]
υ	kinematic viscosity of fluid [m^2s^{-1}]
Φ	inclination angle [deg]

***Corresponding Author:** Ahmed Kadhim Hussein, Department of Mechanical Engineering, College of Engineering, University of Babylon, Babylon Province, Iraq. ahmedkadhim7474@gmail.com (A. K. Hussein)

1. INTRODUCTION

Buoyant MHD flows occur, among other problems, in liquid metal blankets for nuclear fusion. Such flows present a great complexity since buoyant, viscous, inertia and MHD forces all play a role, and analytical or asymptotic solutions are known only for the simplest configurations [1]. In addition, the application of a magnetic field in various research areas has significantly increased in recent years. The development of super-conducting magnets has allowed the generation of magnetic fields up to 20 T (or higher with hybrid magnets) as reported by Teamah [2].However, due to the development of superconducting magnets, a new phenomenon called magnetic convection could be investigated. Braithwaite *et al.* [3] was the first researcher reported the influence of magnetic field on the natural convection of a paramagnetic fluid. Many investigators studied the simple rectangular and square cavities with temperature gradient experimentally and numerically. A good review was reported by Ostrach [4]. Ozoe and Okada [5] conducted a numerical analysis of the magnetic damping effect in a cubic cavity with two vertical walls at different temperatures. They found that the strongest damping effect was achieved with the magnetic field applied perpendicular to the hot wall. Tagawa *et al.* [6] employed a similar way to Boussinesq approximation for the magnetic force and carried out numerical analysis for natural convection of air in a cubic enclosure. Kaneda *et al.* [7] studied natural convection in a cubic enclosure filled with air. The cube was heated from above and cooled from bottom and the air was driven by a magnetic force. Experimental investigation of the thermally induced convection of molten gallium in magnetic fields was carried out by Xu *et al.* [8]. Seki *et al.* [9] studied the laminar natural convection of mercury subjected to a magnetic field parallel to gravity in a rectangular enclosure. Numerical results were found and compared to their experiment with which considered a partially heated vertical wall by a uniform heat generator. Rudraiah *et al.* [10] performed a numerical simulation about natural convection in a two-dimensional cavity filled with an electrically conducting fluid in the presence of a magnetic field aligned to gravity. They selected both Grashof and Hartmann numbers as controlling parameters to examine the effect of a magnetic field on free convection and associated flow dynamics.

Recently, many researchers have taken an interest of the studying of magnetic convection in complex geometries of enclosures, by reason of its great importance in industrial fields. In fact, the study of heat transfer near irregular surfaces is of fundamental importance; that is because it is often met in many practical applications and devices such as flat-plate solar collectors and flat-plate condensers in refrigerators. The presence of roughness elements disturbs the flow past surfaces and alters the heat transfer rate. Yao [11] examined the natural convection heat transfer from isothermal vertical wavy surfaces, such as sinusoidal surfaces, in Newtonian fluids. He proposed a simple transformation to study the natural convection heat transfer from isothermal vertical wavy surfaces. Hady *et al.* [12] analyzed the problem of MHD free convection flow along a vertical wavy surface in presence of magnetic field and generation absorption. Berrahil and Bessaih [13] studied the magnetohydrodynamics stability oscillatory natural convection in a cylindrical enclosure filled with liquid metal whose Prandtl number equals to 0.015, having an aspect ratio equals to 2, and subjected to an axial temperature gradient and a constant magnetic field. The finite volume method was used in order to solve the governing equations. The results showed the dependence of the critical Grashof number with the increase of the Hartmann number. Ece and Buyuk [14] carried out numerical study of steady, laminer natural convection flow in the presence of a magnetic field in an inclined rectangular enclosure heated from one side and cooled from the adjacent side. The results showed that the orientation and the aspect ratio of the enclosure and the strength and the direction of the magnetic field had significant effects on the flow and temperature fields. They concluded that the circulation inside the enclosure became stronger as the Grashof number increased, while the magnetic field suppressed the convective flow and the heat transfer rate. Al-Najem *et al.* [15] numerically investigated the effect of the transverse magnetic field on flow field patterns and heat transfer processes in a tilted square cavity. The horizontal walls of the enclosure were considered to be insulated while the vertical walls were kept isothermal. The power law control volume approach was developed to solve the conservation equations at Prandtl number of 0.71. The study covered the range of the Hartmann number from 0 to 100, the enclosure inclination angle from 0° to -90° with Grashof number of 10^4 and 10^6. The effect of the magnetic field was found to suppress the convection currents and heat transfer inside the cavity. This effect was significant for low inclination angles and high Grashof numbers. Additionally, it was noted that there was no variation of average Nusselt number with respect to inclination angle for high Hartmann number.

Cowley [16] investigated two-dimensional flow driven by buoyancy forces in tilted rectangular enclosures for the case of high Hartmann number and high interaction parameter. Two of the bounding walls were taken to be thermally insulated and the other two to have a constant heat flux. Ece and Buyuk [17] considered steady, laminar, natural-convection flow in the presence of a magnetic field in an inclined square enclosure differentially heated

along the bottom and left vertical walls while the other walls were kept isothermal. The results explained that the orientation of the enclosure changed the temperature gradient and had a significant effect on the flow pattern. Also, they noticed that the magnetic field suppressed the convective flow and its direction also influenced the flow pattern, causing the appearance of inner loops and multiple eddies. Venkatachalappa and Subbaraya [18] presented a numerical study for magnetohydrodynamic free convection of an electrically conducting fluid in a two-dimensional rectangular enclosure in which two side walls were maintained at uniform heat flux condition. The horizontal top and bottom walls were thermally insulated. Computations were carried out over a wide range of Grashof number and Hartmann number for an enclosure of aspect ratio 1 and 2. Numerical results showed that with the application of an external magnetic field, the temperature and velocity fields were significantly modified. When the Grashof number was low and the Hartmann number was high, the central streamlines were elongated and the isotherms were almost parallel representing a conduction state. For sufficiently large magnetic field strength, the convection was suppressed for all values of Grashof number. The average Nusselt number decreased with an increase of Hartmann number and hence a magnetic field can be used as an effective mechanism to control the convection in an enclosure. Saha *et al.* [19] studied numerically a two-dimensional, steady and laminar viscous incompressible flow in a sinusoidal corrugated inclined enclosure. In their analysis, two vertical sinusoidal corrugated walls were maintained at a constant low temperature whereas a constant heat flux source whose length was varied from 20 to 80% of the total length of the enclosure was discretely embedded at the bottom wall. Results were presented in the form of streamline and isotherm plots. It was concluded that the average Nusselt number increased as inclination angle increased for different heat source sizes. Further investigation of natural convection on the same geometry was recently performed by Saha [20], where he analyzed the effect of magnetic field on heat transfer without considering any inclination effects. It was useful to mention that a wide knowledge of the magnetic field effect on engineering processes was described in a book by Ozoe [21].

Motivated by the works mentioned above a steady, laminar, magneto-hydrodynamic natural convection problem has been solved for sinusoidal corrugated inclined enclosure and liquid gallium, whose Prandtl number is fixed to be 0.02, has been taken as a working fluid. The corrugation geometry and the coordinate systems are shown in Fig. 1. A Cartesian coordinate is used with origin at the lower left corner of the computational domain. The geometry consists of a wavy corrugated square enclosure of dimensions, ($W \times W$). The shape of the wavy side walls is taken as sinusoidal. In the present paper, two sidewalls are maintained at a constant temperature T_c, a constant flux heat source, q of length L is discretely embedded at the bottom wall, and the remaining parts of the bottom wall and the upper wall are considered to be thermally insulated. The corrugated wall has a single corrugation frequency and the corrugation amplitude has been fixed at 10% of the enclosure length. The effects of various orientations on the heat transport process inside the sinusoidal corrugated enclosure are studied in the present work. The ratio of the size of the heating element to the enclosure width, $\varepsilon = L/W$ is varied from 0.2 to 0.8 and the inclination angle of the enclosure (Φ), with the horizontal is varied from 0° to 45° in steps of 15°. The Rayleigh number, Ra is varied from 10^3 to 10^6 while Hartmann number, Ha is varied from 0 to 100. The velocity and temperature fields inside the enclosure are presented in terms of a streamline and an isotherm maps and the effects of the magnetic field strength on transport phenomena are discussed.

2. MATHEMATICAL ANALYSIS

A steady two-dimensional magneto-hydrodynamic convective flow in an inclined sinusoidal corrugated square enclosure filled with an electrically conducting fluid is considered. The fluid properties are also assumed to be constant, except for the density in the buoyancy term, which follows the Boussinesq approximation. The gravity acts vertically downwards. A uniform external magnetic field B_o is applied perpendicularly to the left side wall. The fluid within the enclosure is assumed Newtonian while the effects of viscous dissipation, radiation and Joule heating are neglected. The viscous incompressible flow and the temperature distribution inside the enclosure are described by the Navier-Stokes and the energy equations, respectively. Under the above assumptions, the governing equations in terms of non-dimensional form as follows (Ece and Buyul [17]):

$$\frac{\partial U}{\partial X}+\frac{\partial V}{\partial Y}=0 \tag{1}$$

$$U\frac{\partial U}{\partial X}+V\frac{\partial U}{\partial Y}=-\frac{\partial P}{\partial X}+Pr\left(\frac{\partial^2 U}{\partial X^2}+\frac{\partial^2 U}{\partial Y^2}\right)+Ra\,Pr\,\theta\,sin\left(\Phi\right) \tag{2}$$

$$U\frac{\partial V}{\partial X}+V\frac{\partial V}{\partial Y}=-\frac{\partial P}{\partial Y}+Pr\left(\frac{\partial^2 V}{\partial X^2}+\frac{\partial^2 V}{\partial Y^2}\right)+Ra\,Pr\,\theta\cos(\Phi)-Ha^2\,Pr\,V \quad (3)$$

$$U\frac{\partial \theta}{\partial X}+V\frac{\partial \theta}{\partial Y}=\frac{\partial^2 \theta}{\partial X^2}+\frac{\partial^2 \theta}{\partial Y^2} \quad (4)$$

where U and V are the dimensionless velocity components in the X and Y directions, respectively, θ is the dimensionless temperature, P is the non-dimensional pressure. The effect of the electromagnetic field is introduced into the momentum equations (3)-(4) through the Hartmann number (*Ha*) which is defined as (Ece and Buyul [17]):

$$Ha=B_o W\sqrt{\frac{\sigma_e}{\mu}}$$

where σ_e is the electrical conductivity and μ is the dynamic viscosity. The other two important non-dimensional governing parameters appeared in Eqs. (2) and (3) are the Rayleigh number (*Ra*) and the Prandtl number (*Pr*) respectively and they are defined as:

$$Ra=\frac{g\beta qW^4}{k\upsilon\alpha} \qquad \text{and} \qquad Pr=\frac{\upsilon}{\alpha}$$

where k is the thermal conductivity of the fluid, g is the gravitational acceleration, β is the volumetric coefficient of thermal expansion, υ is the kinematic viscosity and α is the thermal diffusivity. The dimensionless parameters used in the governing equations (1-4) are expressed in the following forms:

$$X=\frac{x}{W},Y=\frac{y}{W},U=\frac{uW}{\alpha},V=\frac{vW}{\alpha},P=\frac{pW^2}{\rho\alpha^2},\theta=\frac{T-T_c}{(qW/k)}$$

Non-dimensional forms of the boundary conditions for the present problem are specified as follows:

All walls: $U = 0$, $V = 0$, Top wall: $\dfrac{\partial\theta}{\partial Y}=0,$ Right and left side walls: $\theta = 0$,

Bottom wall: $\dfrac{\partial\theta}{\partial Y}=\begin{cases}0 & for \quad 0<X<0.5(1-\varepsilon) \ and \ \ 0.5(1+\varepsilon)<X<1\\ -1 & for \quad 0.5(1-\varepsilon)\le X\le 0.5(1+\varepsilon)\end{cases}$

The averaged Nusselt number (*Nu*) at the heated surface can be written as (Saha *et al.* [19]):

$$Nu=\frac{1}{\varepsilon}\int_0^{\varepsilon}\frac{1}{\theta_S(X)}dX$$

where $\theta_s(X)$ is the local dimensionless temperature of the heated surface, The Simpson's 1/3 rule is used for numerical integration to obtain the average Nusselt number.

3. NUMERICAL PROCEDURE

The numerical technique used in the present study is similar to that of Hortmann *et al.* [22] based on the finite-volume method (FVM). The solution domain is first subdivided into a finite number of control volumes (CV) where non-orthogonal grids are used. The grid generation calculation is applied to fluid flow. Grids are oriented in such a way that the number of CV is higher near the walls where higher gradients of variable values are expected. A collocated variable arrangement is used in the present investigation. All variables are calculated at the center of each CV. The SIMPLE algorithm is chosen to numerically solve the governing differential equations in their primitive form. The pressure correction equation is derived from the continuity equation to enforce the local mass balance. First, the momentum equations, Eqs. (2-3) are discretized and linearized. Central differencing is used to discretize the diffusion terms, whereas a blending of upwind and central differencing is used for the convection terms. The source terms in the governing transport equations are functions of the respective transported variables and are calculated implicitly. Linear interpolation and numerical differentiation are used to express the cell-face value of the variables and their derivatives through the nodal values. Discretized momentum equations lead to an algebraic system of equations for velocity components U and V where pressure, temperature, fluid properties are taken from the previous iteration except the first iteration where initial conditions are applied. These linear equation systems are solved iteratively (inner iteration) to obtain an improved estimate of velocity. The improved velocity field is then

used to estimate new mass fluxes, which satisfy the continuity equation. The pressure-correction equation is then solved using the same linear equation solver and the same tolerance. The energy equation is then solved in the same manner to obtain a better estimate of the new solution. This completes one outer iteration and is repeated until the residual level is less than or equal to 10^{-6}. In this study, the SIP (Strongly Implicit Procedure) solver based on lower-upper decomposition [23] is used to solve the linear equation systems. To avoid divergence, an under-relaxation parameter with the value of 0.6 is used for velocity, 0.2 for pressure and 0.85 for temperature.

4. GRID REFINEMENT CHECK

In order to obtain grid independent solution, a grid refinement study is performed for a sinusoidal corrugated enclosure with the flat top and bottom walls and the shape of the wavy side walls is taken as sinusoidal. The same boundary conditions of the current study is considered here with $Ra = 10^6$, $Pr = 0.02$, $Ha = 100$, $\varepsilon = 0.8$ and $\Phi = 45°$. In the present work, eight combinations (40 × 40, 50 × 50, 60 × 60, 70 × 70, 80 × 80, 100 × 100, 120 × 120 and 150 × 150) of non-uniform grids are used to test the effect of grid size on the accuracy of the predicted results. Fig. 2 shows the convergence of the average Nusselt number at the heated Surface of the sinusoidal corrugated enclosure with grid refinement. It is observed that grid independence is achieved with combination of (100 × 100) control volumes where there is insignificant change in *Nu* with improvement of finer grids.

5. VERIFICATION OF RESULTS

In order to make sure that the developed codes are free of error, a validation test is conducted. The present numerical approach is verified against the results published by Pirmohammadi and Ghassemi [24] for natural convection flows with the presence of a longitudinal magnetic field in a tilted square cavity that is heated from below and cooled from the top while other walls are adiabatic. Fig. 3 shows the streamlines and the isotherms calculated by Pirmohammadi and Ghassemi [24] as well as by employing the present code for $Ra = 10^5$, $Pr = 0.02$, $\Phi = 0°, 45°, 90°$ and 135° and $Ha = 0$, 50 and 70 considering the same boundary conditions but the numerical scheme is different. Excellent qualitative agreement is achieved between the results of Pirmohammadi and Ghassemi [24] and that of the present numerical scheme for both flow and thermal fields over the range of governing parameters. This validation makes a good confidence in the present numerical model to deal with the physical problem. Moreover, a quantitative agreement is made by comparing the results of the present numerical model with those reported by Corvaro and Paroncini [25], for square straight enclosure with different Raleigh number and $\varepsilon = 0.2$ as shown in Table 1. The comparison with those experimental data is found to be excellent which validates the present computations indirectly.

6. RESULTS AND DISCUSSION

In this research, a numerical study is carried out numerically for different discrete heat source size ratios $\varepsilon = 0.2, 0.4, 0.6$ and 0.8, inclination angles of the sinusoidal corrugated enclosure $\Phi = 0^o, 15^o, 30^o$ and 45^o, Rayleigh number, $Ra = 10^3, 10^4, 10^5$ and 10^6 and Hartmann number, $Ha = 0, 25, 50, 75$ and 100.

The main characteristics of the flow and the heat transport for sinusoidal corrugated horizontal enclosure ($\Phi = 0^o$) are shown in Figs. 4 and 5 in terms of streamline and isotherm plots respectively for various values of *Ra* ranging from 10^3 to 10^6 and *Ha* from 0 to 100 with a discrete heat source size ratio of 0.2. Because of the symmetrical boundary conditions on the sinusoidal corrugated sidewalls, the temperature fields are almost symmetric about the vertical mid-plane of the enclosure, whereas the flow fields are asymmetric due to wavy sidewalls. The symmetrical boundary conditions in the vertical direction cause to produce a couple of asymmetrical anticlockwise and clockwise rotating cells in the left and the right halves of the enclosure. In most of the cases, the flow rises along the vertical center line from the middle part of the bottom wall and gets blocked at the top adiabatic wall, which turns the flow horizontally towards the isothermal cold sidewalls. After that, the flow moves downwards along the sinusoidal corrugated sidewalls and turns back horizontally to the central region after hitting the bottom wall. With the increase of Hartmann number, the viscous forces become more dominant than the buoyancy forces and the inner of the two symmetrical circulating cells of almost equal strength is directed towards the end points of the heat source. On the other hand, the isotherm graphs are nearly symmetric about the vertical centre line of the enclosure and the shape of the streamlines tend to follow the geometry of the enclosure as shown in Fig. 5; so heat transfer is essentially diffusion dominated. The temperature decreases from the bottom hot wall to the top adiabatic wall along the vertical centre line of the enclosure and concentrates towards the hot bottom wall indicating the existence of a large temperature gradient. Near the sidewalls of the enclosure, the isotherms are almost symmetrical, while the isotherms

in the middle of the enclosure take the shape of smooth curves which are symmetric with respect to the vertical mid-plane of the enclosure. For high Rayleigh number, where buoyancy forces are more dominant than the viscous forces, the convection currents inside the enclosure become very strong. Since the cold fluid has a downward motion with an increase of circular flow, the convection becomes the basic mode of heat transfer. In this case, the anticlockwise and the clockwise rotating cells move up and become irregular in shape. Also, the isotherm pattern changes significantly. With the increase of Rayleigh number, the developing thermal boundary layer thickness at the bottom wall becomes thinner and thus refers high heat transfer rate. On the other hand, distortion of isotherms plots is reduced significantly with the increase of Hartmann number. The flow fields also take the shape of two circulating cells of same size from one dominated circulating cells at the center of the enclosure.

The flow and the heat transport for sinusoidal corrugated geometry of heat source size ratio (ε) of 0.2, 0.4, 0.6 and 0.8 are shown in Figs. 6 and 7 for different values inclination angles while keeping *Ra* (= 10^6) and *Ha* (= 0) are fixed. When $\Phi = 0^o$ and $\varepsilon = 0.2$, a large rotating cell along with a couple of small eddies of opposite direction of motion occupy the whole cavity as mentioned earlier. When the inclination angle increases from 0^o to 15^o, the minor cell at lower right corner becomes smaller and further increases of tilt angle eventually allows the main circulating cell to be dominant which in turns spreads inside the sinusoidal corrugated enclosure. This results in higher recirculation strength and convection current becomes the dominant mode of heat transfer. With this high value of *Ra* and zero magnetic effect, the flow field is affected by a large rotating cell and becomes identical irrespective of discrete heat source size ratio. A careful observation near the bottom left corner indicate that due to the sinusoidal side wall, the flow gets entrapped by the local minor eddies in both clock wise and anti-clockwise direction. Now when the heat source size increases, the small clockwise rotating cell at the lower left corner expands, thus squeezing the small right circulating cell. At the inclination angle of 45^o, the large circulating cell covers most parts of the sinusoidal corrugated enclosure with a large magnitude of circulation which indicates increasing the buoyancy effect. It then becomes dominating near the heat source while the small right circulating cell decreases in size and in general allows the main flow to move closer to the heat source. Moreover, at $\Phi = 45^o$ a small minor cell is observed at the top corner of the left cold sidewall and the overall pattern of the stream lines on the upper part of the cavity is same as shown in Fig. 6. Now observing the isothermal profiles in Fig. 7, it is found that the angle of inclination as well as discrete heat source size ratio has noticeable effect on the heat transfer characteristics. At high Rayleigh and zero Hartmann number, the isotherm plots with temperature contours, $\theta = 0 - 0.03$ occur asymmetrical about the vertical mid-plane of the enclosure. For low inclination angle ($\Phi \leq 15^o$) and $\varepsilon = 0.2$, the temperature contours noticeably $\theta = 0.02$ move slightly from left to right and with the increase of inclination angle ($\Phi \geq 30^o$), the isotherms are pushed towards the lower part of the right sidewall due to the expansion of main circulating cell. This behavior can be noticed at high heat source size ratio with different inclination angles. When $\varepsilon = 0.8$, the temperature contours are continuously compressed towards the cold right sidewall. As the non-linearity of the isotherms increases, the existence of a thin thermal boundary layer clusters near the lower part of the right sidewall with the increase of Φ. The reason of these phenomena is due to the division of the buoyancy force in both *x*- and *y*-directions. It is noteworthy to mention that increasing size of discrete heat source momentarily increases the maximum temperature inside the cavity and the small temperature gradient observed near the boundary layer produces low circulation of fluid flow inside the cavity. In all these cases, the convective current is responsible for the heat transfer mechanism due to the higher value of Rayleigh number.

Figures 8(a), (b) and (c) depicts the variation of the average Nusselt numbers along the heated strip at the bottom wall with Rayleigh number from 10^3 to 10^6 for different values of Hartmann number, discrete heat source size ratio and enclosure inclination angle respectively. From these figures, it is observed that at any particular corrugated geometry with or without the presence of magnetic field, the average Nusselt number does not change up to *Ra* = 10^4 and then it increases significantly with the increasing of Rayleigh number due to convection dominated heat transfer. Additionally, it is noticed that there is no variation of average Nusselt number until *Ra* = 10^5 for *Ha* $\geq$ 50. This is consistent with the results of Ece and Buyuk [14], Al-Najem *et al.* [15] and Ece and Buyuk [17]. As the magnetic field has a tendency to suppress the convective flow and heat transfer inside the cavity as observed in their results [14, 15, 17], similar pattern of average Nusselt number profiles for a sinusoidal enclosure confirms the influence of magnetic field on the thermal performance. The effects of discrete heat source size ratio on *Nu* without the presence of magnetic field (*Ha* = 0) at an inclination angle of 45^o is presented in Fig. 8(b). It is observed that the heat transfer rate decreases with the increase of heat source size and the smaller size ratio produces the maximum value of Nusselt number for any value of Rayleigh number. Similar to the observation of Saha *et al.* [19], it is also concluded from Fig. 8(c) that the average Nusselt number significantly increases as the inclination angle increases to a certain value for low Rayleigh number. When the Rayleigh number increases from 10^4 to 10^6, the rate of increase of *Nu* with the change of inclination angles drops drastically.

Table 1. Comparison of average Nusselt number between the experimental and the numerical works for $\varepsilon = 0.2$

Ra	Average Nusselt number		
	Experimental results of Corvaro and Paroncini [25]	Present numerical results (FVM)	Error (%)
7.56×10^4	4.8	5.135	-6.97
1.38×10^5	5.859	5.863	-0.06
1.71×10^5	6.3	6.235	1.03
1.98×10^5	6.45	6.385	1.00
2.32×10^5	6.65	6.571	1.18
2.50×10^5	6.81	6.669	2.07

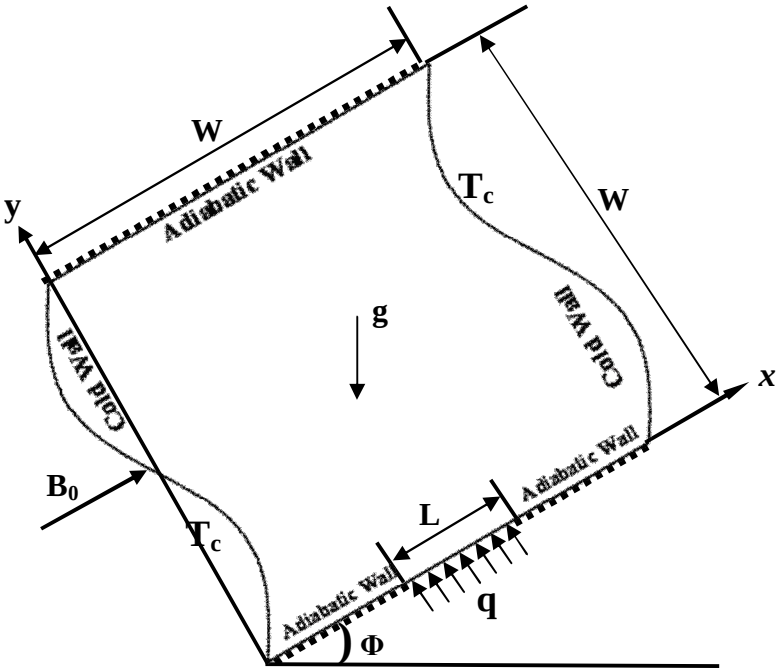

Fig. 1: Schematic configuration of the tilted sinusoidal corrugated cavity with coordinate system along with boundary conditions and longitudinal magnetic effect

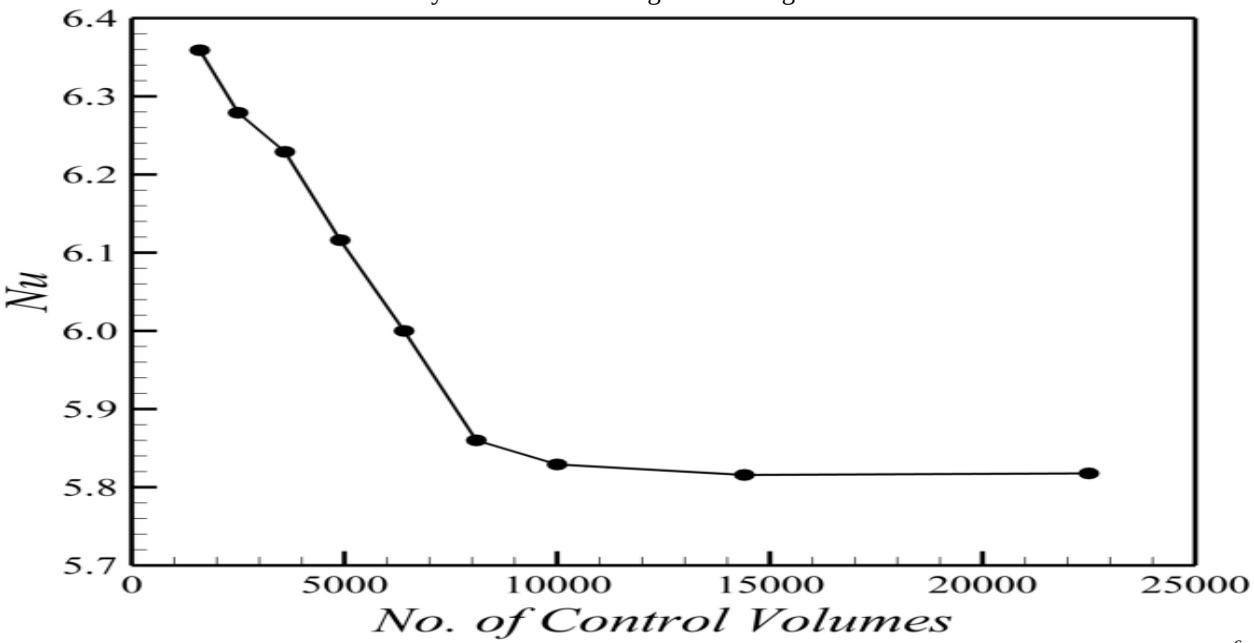

Fig. 2: Convergence of average Nusselt number (*Nu*) along the heated bottom wall with grid refinement at $Ra = 10^6$, $Ha = 100$, $Pr = 0.02$, $\varepsilon = 0.8$ and $\Phi = 45°$

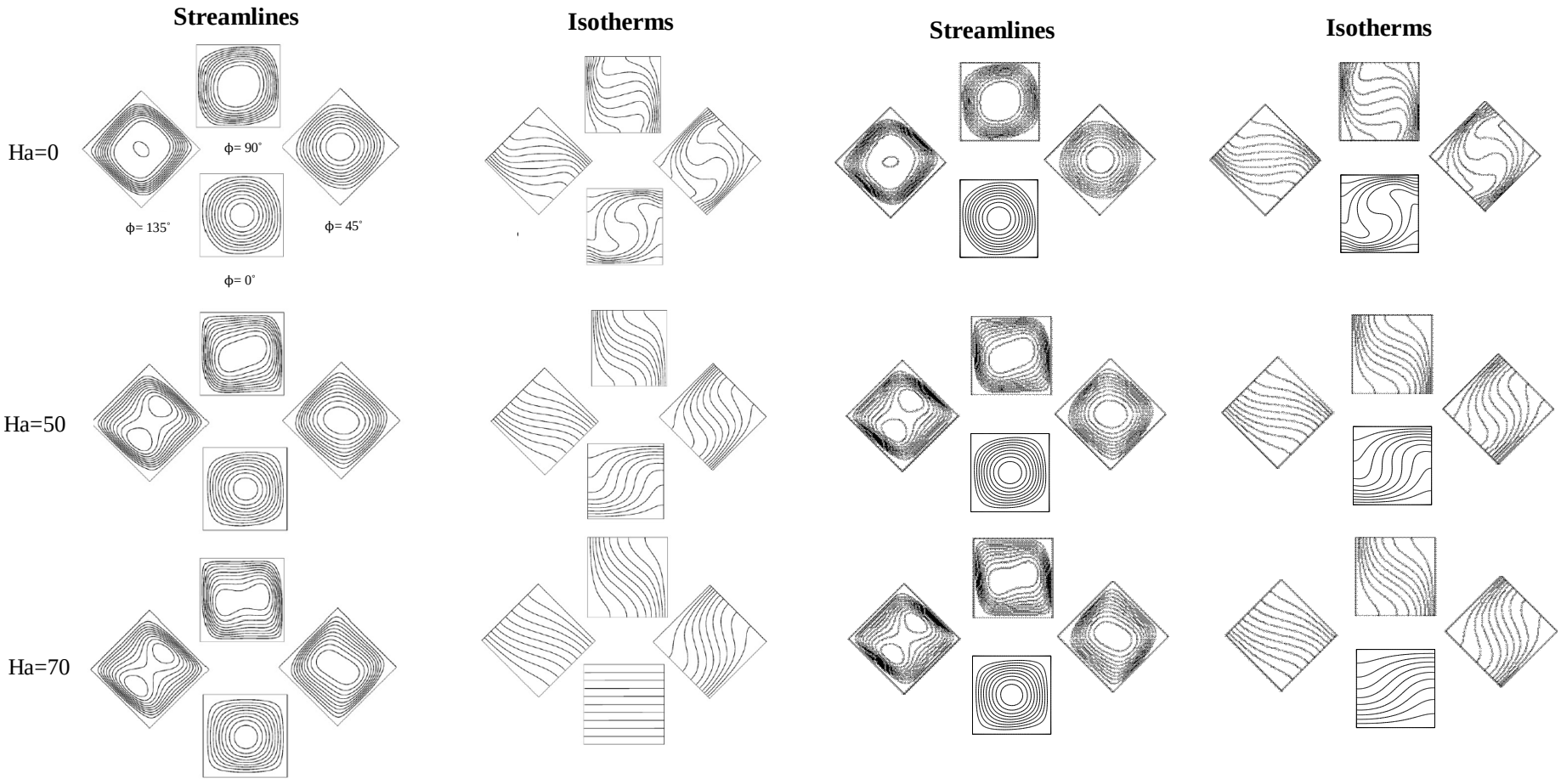

Fig. 3: Comparison of the streamlines and the isotherms at different inclination angles (Φ) and Hartmann numbers (Ha) between the results obtained by the present code (right) and that of Pirmohammadi and Ghassemi [24] (left) for $Pr = 0.02$ and $Ra = 10^5$.

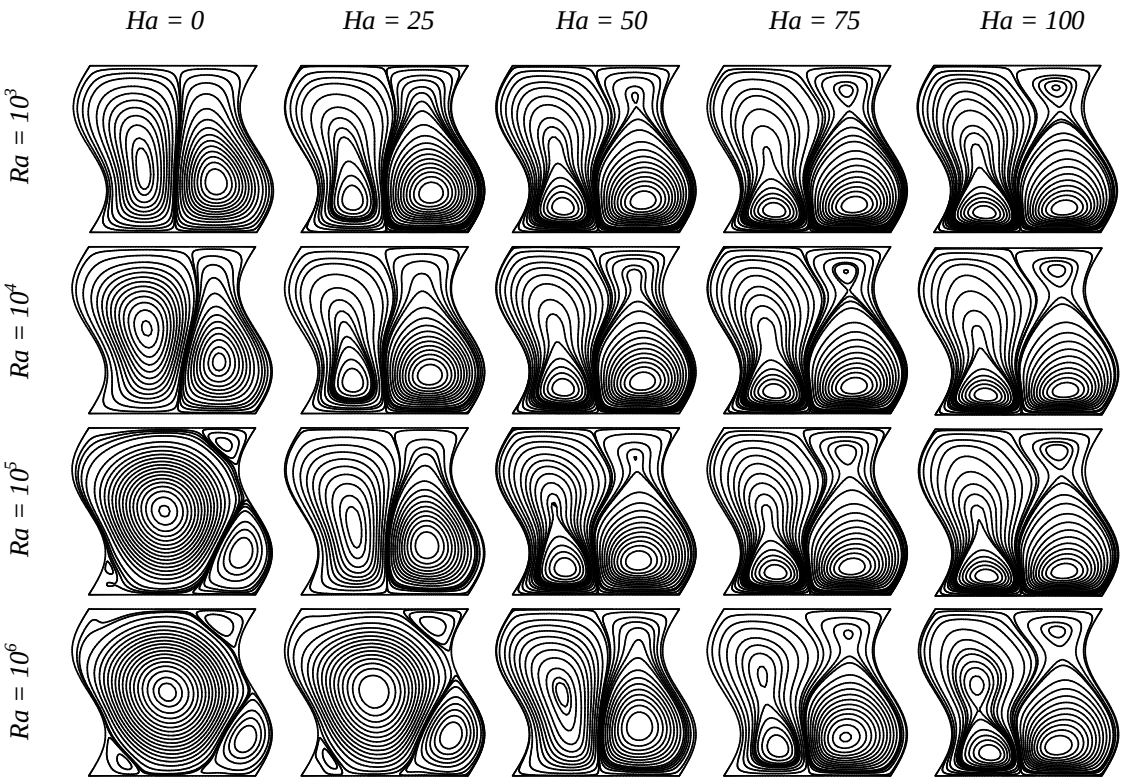

Fig. 4: Streamlines for different Hartmann numbers (*Ha*) and Rayleigh numbers (*Ra*) with $\varepsilon = 0.2$ and $\Phi = 0^{\circ}$.

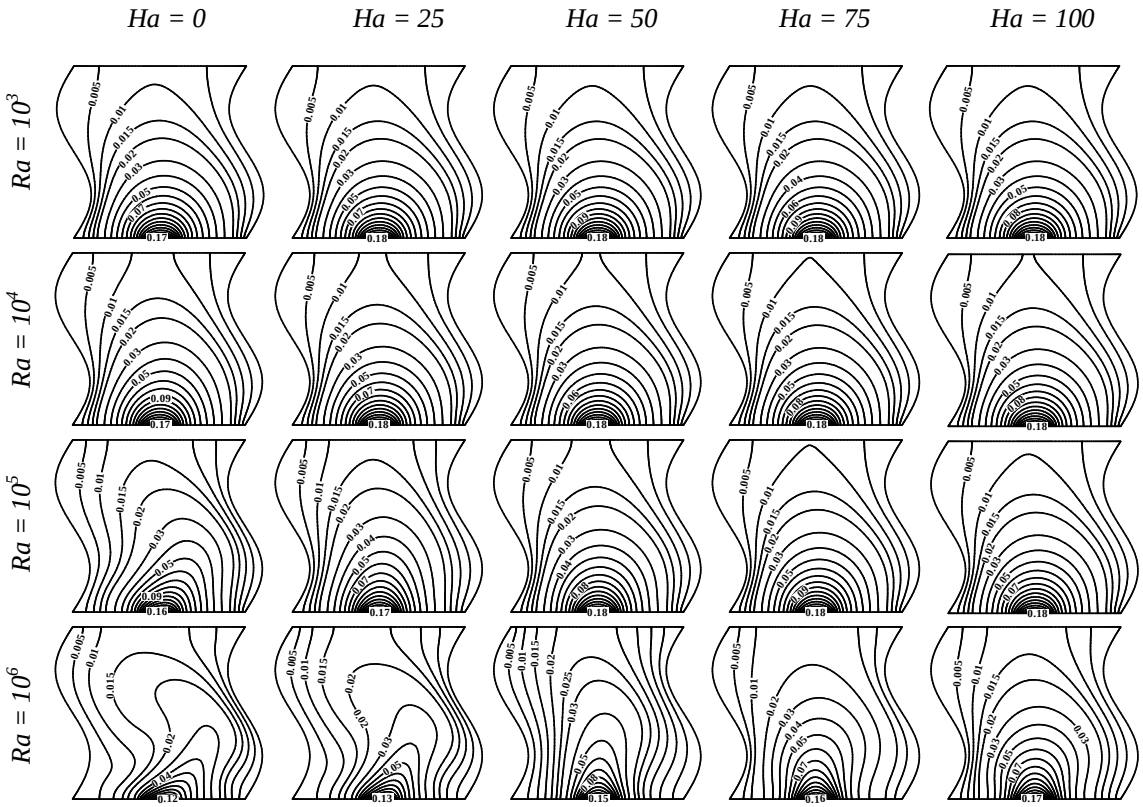

Fig. 5: Isotherms for different Hartmann numbers (*Ha*) and Rayleigh numbers (*Ra*) with $\varepsilon = 0.2$ and $\Phi = 0^{o}$.

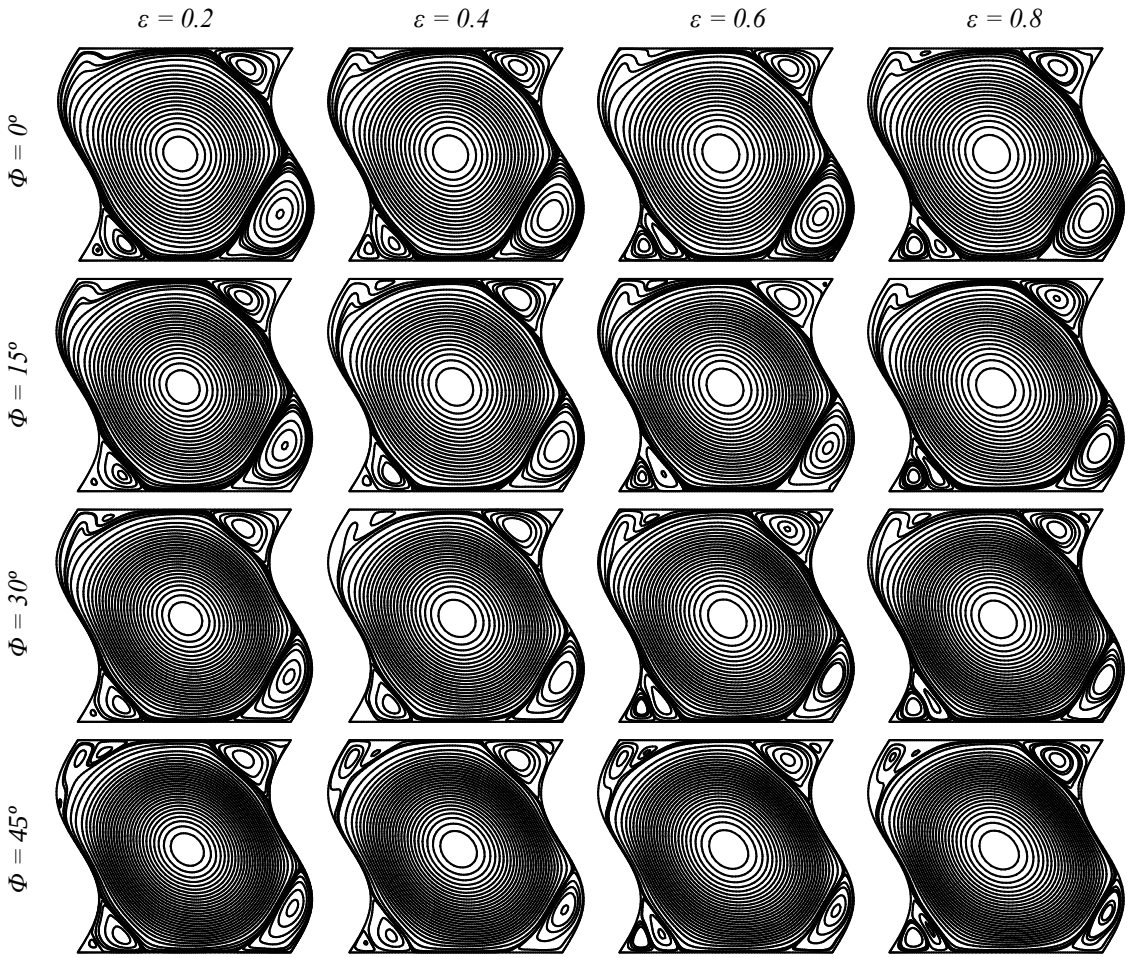

Fig. 6: Streamlines for different discrete heat source size ratios (ε) and inclination angles (Φ) with $Ha = 0$ and $Ra = 10^6$.

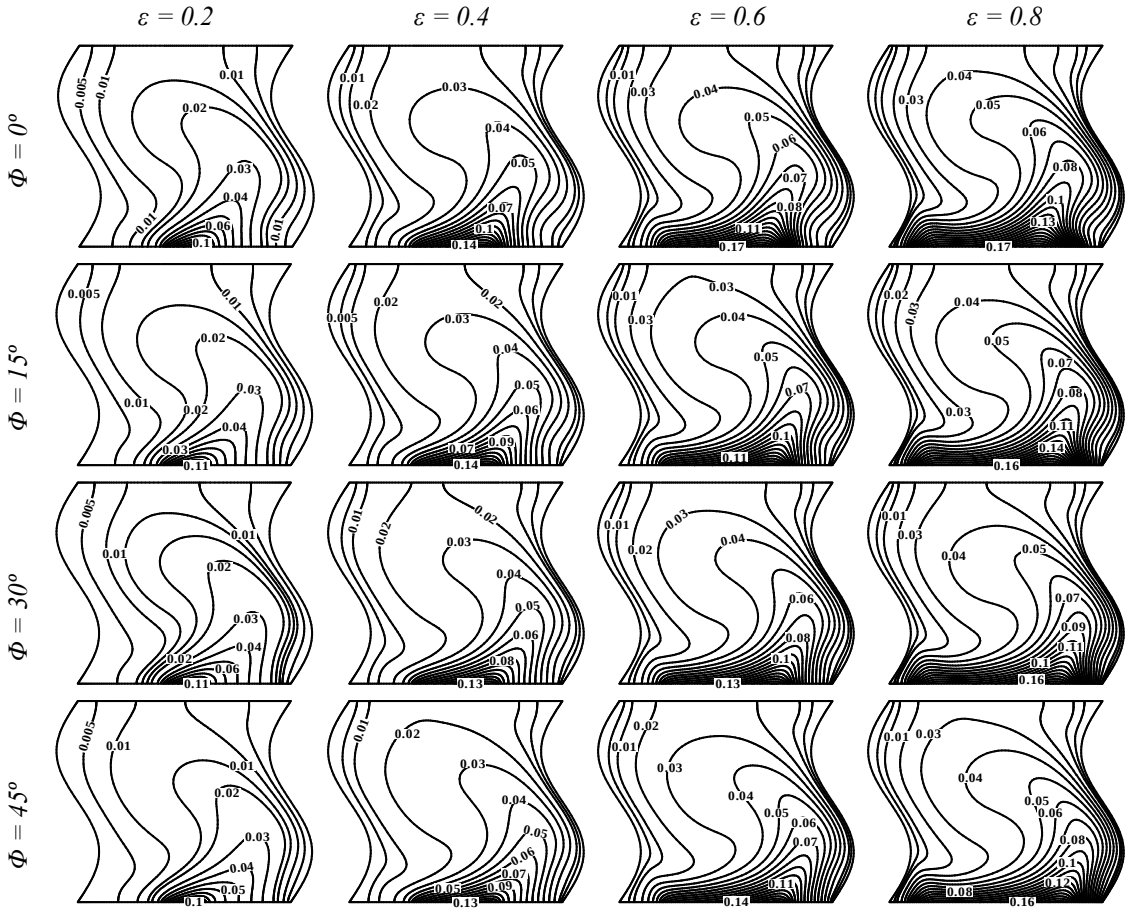

Fig. 7: Isotherms for different discrete heat source size ratios (ε) and inclination angles (Φ) with $Ha = 0$ and $Ra = 10^6$.

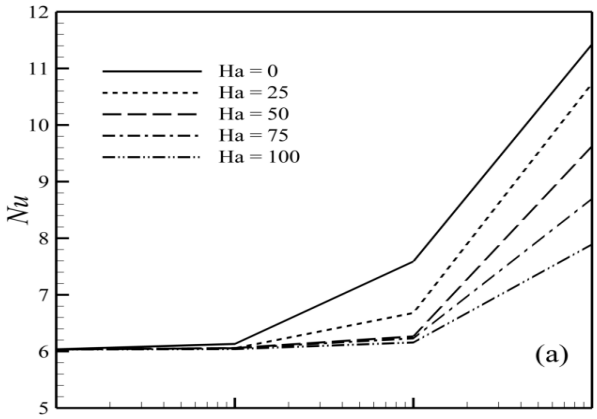

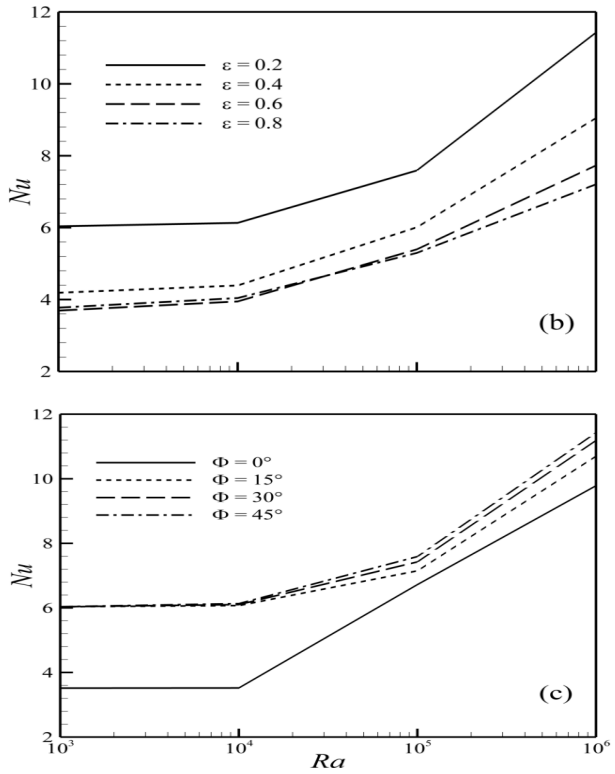

Fig. 8: Variation of the average Nusselt number (*Nu*) with Rayleigh number (*Ra*) along with (a) different Hartmann numbers (*Ha*) for $\Phi = 45^{o}$ and $\varepsilon = 0.2$, (b) different discrete heat source size ratios (ε) for $\Phi = 45^{o}$ and *Ha* = 0 and (c) different enclosure inclination angles (Φ) for *Ha* = 0 and $\varepsilon = 0.2$.

7. CONCLUSIONS

The effect of cavity inclination angle, longitudinal magnetic field and discrete is flux heat source size on natural convection inside a sinusoidal corrugated enclosure are investigated and analyzed in this study. The finite volume method helps to obtain numerical solution in terms of stream functions and temperature contours for $Ra = 10^3$ to 10^6 and $Pr = 0.02$. From the above discussion, following conclusions can be drawn:

(i) The application of a longitudinal magnetic field results in a force opposite to the flow direction that leads to drag the flow and then reduces the convection currents by reducing the velocities.

(ii) For low Rayleigh number and high Hartmann number, diffusion is the basic mode of heat transfer which results the minimum value of thermal performance from the heated wall. On the other hand, with the increase of Rayleigh number, the thermal boundary layer thickness decreases and it would become thinner when the effect of Hartmann number is going to cease on the flow and the thermal fields. Then convection becomes the main mode of heat transfer which in turns enhances the performance of heat transfer inside the sinusoidal enclosure.

(iii) The average Nusselt number increases significantly with the increase of Rayleigh number and the decrease of Hartmann number and hence a magnetic field can be used as an effective mechanism to control the convection inside an enclosure.

(iv) The average Nusselt number also increases as the discrete heat source size decreases and vice verse. The enclosure inclination angle has a clear effect on the heat transfer process as well. It is found that for small size of discrete heat source, the values of *Nu* increases significantly as soon as the cavity orientation changes from horizontal to any inclined position. Moreover, the effect of change of inclination angle on heat transfer is only dominant at higher value of Rayleigh number.

8. REFERENCES

[1] L. Bühler, Laminar buoyant MHD flow in vertical rectangular ducts, J. Physics Fluids 10 (1998) 223-236.

[2] M. A. Teamah, Hydro-magnetic double-diffusive natural convection in a rectangular enclosure with imposing an inner heat source or sink, Alexandria Engineering J. 45 (2006) 401-415.
[3] D. Braithwaite, E. Beaugnon, R. Tournier, Magnetically control-led convection in a paramagnetic fluid, Nature 354 (1991) 134-136.
[4] S. Ostrach, Natural convection with combined driving forces, Physico Chemical Hydrodynamics 1 (1980) 233–247.
[5] H. Ozoe, K. Okada, The effect of the direction of the external magnetic field on the three-dimensional natural convection in a cubic enclosure, Int. J. Heat Mass Transfer 32 (1989) 1939–1953.
[6] T. Tagawa, R. Shigemitsu, H. Ozoe, Magnetizing force modeled and numerically solved for natural convection of air in a cubic enclosure: effect of the direction of the magnetic field, Int. J. Heat Mass Transfer 45 (2002) 267–277.
[7] M. Kaneda, T. Tagawa, H. Ozoe, Convection induced by a cuspshaped magnetic field for air in a cube heated from above and cooled from below, J. Heat Transfer 124 (2002) 17–25.
[8] B. Xu, B. Li, D. Stock, An experimental study of thermally induced convection of molten gallium in magnetic fields, Int. J. Heat Mass Transfer 49 (2006) 2009 –2019.
[9] M. Seki, H. Kawamura, K. Sanokawa, Natural convection of mercury in a magnetic field parallel to the gravity, J. Heat Transfer 101 (1979) 227–232.
[10] N. Rudraiah, R. Barron, M. Venkatachalappa, C. Subbaraya, Effect of a magnetic field on free convection in a rectangular enclosure, Int. J. Engng. Sci. 33(8) (1995) 1075–1084.
[11] L. Yao, Natural convection along a vertical wavy surface, J. Heat Transfer 105 (1983) 465-468.
[12] F. Hady, R. Mohamed, A. Mahdy, MHD free convection flow along a vertical wavy surface with heat generation or absorption effect, Int. Comm. Heat Mass Transfer 33 (2006) 1253-1263.
[13] F. Berrahil, R. Bessaih, Magnetohydrodynamic stability of oscillatory natural convection in a cylindrical enclosure filled with liquid metal, World J. Engg. 5 (2008) 1-9.
[14] M. Ece, E. Buyuk, Natural convection flow under a magnetic field in an inclined rectangular enclosure heated and cooled on adjacent walls, Fluid Dynamics Research 38 (2006) 546-590.
[15] N. Al-Najem, K. Khanafer, M. El-Refaee, Numerical study of laminar natural convection in tilted enclosure with transverse magnetic field, Int. J. Numerical Methods Heat Fluid Flow 8(6) (1998) 651-672.
[16] M. Cowley, Natural convection in rectangular enclosures of arbitrary orientation with magnetic field vertical, Magnetohydrodynamics 32 (1996) 390-398.
[17] M. Ece, E. Buyuk, Natural convection flow under a magnetic field in an inclined square enclosure differentially heated on adjacent walls, Meccanica 42 (2007) 435-449.
[18] M. Venkatachalappa, C. Subbaraya, Natural convection in a rectangular enclosure in the presence of a magnetic field with uniform heat flux from the side walls, Acta Mechanica 96 (1993) 13-26.
[19] S. Saha, T. Sultana, G. Saha, M. Rahman, Effects of discrete isoflux heat source size and angle of inclination on natural convection heat transfer flow inside a sinusoidal corrugated enclosure, Int. Comm. Heat Mass Transfer 35 (2008) 1288-1296.
[20] G. Saha, Finite element simulation of magnetoconvection inside a sinusoidal corrugated enclosure with discrete isoflux heating from below, Int. Comm. Heat Mass Transfer 37 (2010) 393-400.
[21] H. Ozoe, Magnetic Convection, Imperial College Press, London, UK, 2005.
[22] M. Hortmann, M. Peric, G. Scheuerer, Finite volume multigrid prediction of laminar natural convection: bench-mark solutions, Int. J. Numerical Methods Fluids 11 (1990) 189–207.
[23] H. Stone, Iterative solution of implicit approximations of multidimensional partial differential equations, SIAM J. Numerical Analysis 5 (1968) 530–558.
[24] M. Pirmohammadi, M. Ghassemi, Effect of magnetic field on convection heat transfer inside a tilted square enclosure, Int. J. Heat Mass Transfer 36 (2009) 776–780.
[25] F. Corvaro, M. Paroncini, A numerical and experimental analysis on the natural convection heat transfer of a small heating strip located on the floor of a square cavity, Applied Thermal Engineering 28 (2008) 25–35.